Electronic Supplementary Material (ESI) for New Journal of Chemistry.

Supporting Information

Synthesis, Structures, Antimicrobial Activity and Biosafety Evaluation of Pyridine-2-formaldehyde-N-susbtituted-thiosemicarbazonates of copper(II) †

Mani Kaushal[a], Tarlok S. Lobana[a,**] Lovedeep Nim[b], Jaskamal Kaur[a], Ritu Bala[a*], Geeta Hundal[a], Daljit S. Arora,[b] Isabel Garcia-Santos[c], Courtney E. Duff[d] and Jerry P. Jasinski[d]

[a]*Department of Chemistry, Guru Nanak Dev University, Amritsar-143 005, India;* [b]*Department of Microbiology, Guru Nanak Dev University, Amritsar-143 005, India;* [c]*Departamento de Quimica Inorganica, Facultad de Farmacia, Universidad de Santiago, 15782-Santiago, Spain, and*

[d]*Department of Chemistry, Keene State College, Keene, NH 03435, USA.*

[#]Email address: tarlokslobana@yahoo.co.in (Tarlok Singh Lobana)

S1.Ligands details (HL^1-R, R = Me, Et, Ph)

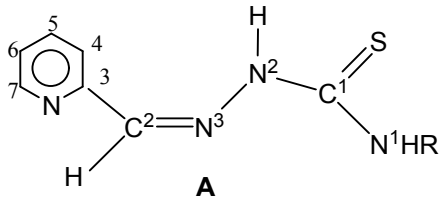

A

S1.1 Preparation of pyridine-2-formaldehyde-N^1-methyl thiosemicarbazone (HL^1-Me)

The solution of 4-methyl-3-thiosemicarbazide (1 g, 9.5 mmol) in methanol was refluxed for 30 minutes at 40˚C. To this solution, pyridine-2-carbaldehyde (0.89 mL) was added along with 2-3 drops of glacial acetic acid and resulting solution was refluxed for seven hours. After that, the solution was left for crystallization at room temperature. M.pt. 240-242 ^oC. 76% Main I.R peaks (KBr, cm^{-1}), $\nu(N^1\text{-}H)$, 3395s, $\nu(N^2\text{-}H)$, 3249s, ν(C-H), 3088w, 3050w,

2955w, ν(C=N) + ν(C=C) 1626s, 1585s, ν(C-N), 1081s, 1031s, ν(C-S), 895s. ^{1}H NMR (DMSO-d^{6}, δ, ppm): 11.63s (1H, -N^{2}H), 8.56(2H; C^{2}H+C^{7}H), 8.20(1H, C^{4}H), 8.03(1H, C^{6}H), 7.79(1H, C^{5}H), 7.33(1H, N^{1}H), 2.98 (3H, -CH_3).

S1.2 Preparation of pyridine-2-formaldehyde-N^{1}-ethyl thiosemicarbazone (HL^{1}-Et)

The solution of 4-ethyl-3-thiosemicarbazide (1 g, 8.4mmol) in methanol was refluxed for 30 minutes at 40˚C. To this, pyridine-2-aldehyde (0.79 mL) was added along with 2-3 drops of glacial acetic acid and resulting solution was refluxed for seven hours. After that, the solution was left for crystallization at room temperature. M.pt. 213-215 °C. Yield 76%. Main I.R peaks (KBr, cm^{-1}), υ(N^{1}-H), 3410s, υ(N^{2}-H), 3260s, υ(C-H) 3060w, 2937w, 2908w, 2868w, υ(C=N) + υ(C=C) 1630s, 1585s, υ(C-N), 1089s, 1051s, υ(C-S) 899s. ^{1}H NMR (DMSO-d^{6}, δ, ppm): 11.58s (1H, -N^{2}H), 8.64, 8.54 (2H; C^{2}H+C^{7}H), 8.32(1H; C^{4}H), 8.04(C^{6}H), 7.80 (1H; C^{5}H), 7.34 (1H; N^{1}H), 3.56(2H; -CH_2) and 1.13 (3H,-CH_3).

S1.3 Preparation of pyridine-2-formaldehyde-N^{1}-phenyl thiosemicarbazone (HL^{1}-Ph)

The solution of 4-phenyl-3-thiosemicarbazide (1 g, 5.9 mmol) in methanol was refluxed for 30 minutes at 40˚C. To this, pyridine-2-aldehyde (0.57 mL) was added along with 2-3 drops of glacial acetic acid and resulting solution was refluxed for seven hours. After that, the solution was left for crystallization at room temperature. M.pt. 204-206 ^{o}C. Yield 72% ; Main I.R. peaks (KBr, cm^{-1}), υ(N^{1}-H), 3415s, υ(N^{2}-H), 3250s, υ(C-H) 3045w, 2915w, 2868w, υ(C=N) + υ(C=C) 1630s, 1585s, υ(C-N), 1089s, 1051s, υ(C-S) 899s. ^{1}H NMR (DMSO-d^{6}, δ, ppm): 11.96s (1H; -N^{2}H), 8.54s(1H; C^{2}H), 8.38(1H; C^{7}H), 8.15(1H; C^{4}H), 7.80-7.16m (8H; N^{1}H +C^{5,6}H+ N^{1}Ph),

S.1.4-6. The ligands 2-benzoylpyridine N-substituted thiosemicarbazones (HL^2-R, R = Me, Et and Ph) and their complexes were prepared as reported earlier.[49] (ref 49 main paper)

S2. X-ray structure and Bond parameters.

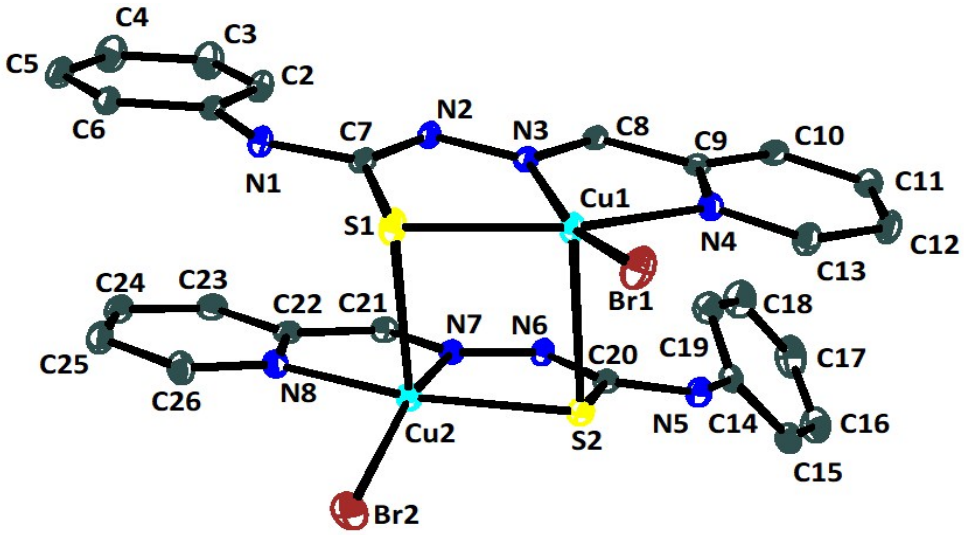

Figure S1. ORTEP diagram of complex $[Cu_2^{II}(\kappa^3:N,N,S\text{-}L^1\text{-}Ph)(\kappa^4:N,N,\mu\text{-}S\text{-}L^1\text{-}Ph)Br_2]$ 6 with 30% ellipsoid probabilty. Cu2-S1 bond is long .

Table S1 Selected bond distances (Å) and bond angles (°) of complexes **2**, **3**, **5**, **6** and **8**

$[Cu_2^{II}(\kappa^2:N,N,\mu\text{-}S\text{-}L^1\text{-}Et)_2I_2]$ **2**			
Cu1–S1	2.273(1)	Cu2-S2	2.272(1)
Cu1-S2	2.778(1)	Cu2- S1	2.709(1)
Cu1–I1	2.591(1)	Cu2-I2	2.598(1)
$Cu1–N1_{(azomethine)}$	1.992(2)	$Cu2\text{-}N6_{(azomethine)}$	1.993(2)
$Cu1–N4_{(pyridyl)}$	2.023(2)	$Cu2\text{-}N5_{(pyridyl)}$	2.028(2)
C-S	1.762(2); 1.763(2)	$C\text{-}N_{(hydrazinic)}$	1.318(3); 1.321(3)

		C-N $_{(amino)}$	1.338(3); 1.333(3)
N4 -Cu1-I1	99.16(6)	N5 -Cu2-I2	98.76(6)
N1$_{(azomethine)}$-Cu1-I1	159.49(6)	N6$_{(azomethine)}$-Cu2-I2	157.42(6)
S1-Cu1-I1	96.23(3)	S2-Cu2-I2	95.63(2)
S1-Cu1-N4$_{(pyridyl)}$	163.59(6)	S2-Cu2-N5$_{(pyridyl)}$	163.67(6)
N4-Cu1-N1	80.47(8)	N5$_{)}$ -Cu2-N6	80.66(8)
S1-Cu1-N1	83.12(6)	S2-Cu2-N6	83.09(6)
Cu1-S1-Cu2	84.62(3)	Cu1-S2-Cu2	83.03(3)
S2-Cu1-S1	93.80(2)	S2-Cu2-S1	95.50(3)
τ value	0.068	τ value	0.104
$[Cu_2^{II}(\kappa^3$:N,N,S-L^1-Ph)(κ^4:N,N,μ-S-L^1-Ph)I_2] **3**			
Cu1-I1	2.5569(8)	Cu2-I2	2.5714(9)
Cu1-N1$_{(pyridyl)}$	2.026(5)	Cu2-N5$_{(pyridyl)}$	2.019(5)
Cu1-N2$_{(azomethine)}$	1.979(5)	Cu2-N6$_{(azomethine)}$	1.977(4)
Cu1–S1	2.2596(16)	Cu2-S2	2.2666(17)
C – S	1.755(6); 1.763(6)	Cu2-S1	2.7993(19)
C-N$_{(hydrazinic)}$	1.311(7); 1.318(8)	C – N $_{(amino)}$	1.339(8); 1.349(8)
N1 -Cu1-I1	99.17(15)	N5 -Cu2-I2	99.40(13)

$N2_{(azomethine)}$-Cu1-I1	158.64(15)	$N6_{(azomethine)}$-Cu2-I2	161.08(15)
S1-Cu1-I1	96.76(4)	S2-Cu2-I2	95.83(5)
$N1_{(pyridyl)}$ -Cu1-S1	163.55(16)	$N5_{(pyridyl)}$-Cu2-S2	163.61(13)
N1-Cu1-N2	81.0(2)	N5-Cu2-N6	80.69(18)
N2-Cu1-S1	82.69(14)	N6-Cu2- S2	82.94(14)
τ value	0.042	S2-Cu2-S1	97.58(6)

$[Cu_2^{II}(\kappa^4:N,N,\mu\text{-}S\text{-}L^1\text{-}Et)_2Br_2]$ **5**

Cu1–S1	2.2705(13)	Cu2-S1	2.7316(12)
Cu1-S2	2.8054(13)	Cu2-S2	2.2642(13)
Cu1–Br1	2.3962(7)	Cu2-Br2	2.4013(7)
$Cu1–N2_{(azomethine)}$	1.992(3)	$Cu2\text{-}N6_{(azomethine)}$	1.990(3)
$Cu1–N3_{(pyridyl)}$	2.028(4)	$Cu2\text{-}N7_{(pyridyl)}$	2.023(4)
C-S	1.757(4);	$C\text{-}N_{(hydrazinic)}$	1.322(6);1.320(5)
	1.749(4)	$C\text{-}N_{(amino)}$	1.332(6);1.337(6)
Br1-Cu1-N3	99.16(10)	Br2-Cu2-N7	98.09(11)
$Br1\text{-}Cu1\text{-}N2_{(azomethine)}$	160.54(10)	$Br2\text{-}Cu2\text{-}N6_{(azomethine)}$	157.67(11)
Br1-Cu1-S1	97.00(4)	Br2-Cu2-S2	96.46(4)
$N3_{(pyridyl)}$-Cu1-S1	163.21(11)	$S2\text{-}Cu2\text{-}N7_{(pyridyl)}$	163.66(11)

N3-Cu1-N2	80.38(15)	N7-Cu2-N6	80.86(15)
N2-Cu1-S1	82.86(11)	S2-Cu2-N6	82.85(11)
Cu1-S1-Cu2	85.51(4)	Cu1-S2-Cu2	83.89(4)
S2-Cu1-S1	92.40(4)	S1-Cu2-S2	94.51(4)
τ value	0.051	τ value	0.099

$Cu_2^{II}(\kappa^3$:N,N,S-L^1-Ph)(κ^4:N,N,μ-S-L^1-Ph)Br_2] **6**

Cu1-Br1	2.3854(4)	Cu2-Br2	2.3614(4)
Cu1-$N4_{(pyridyl)}$	2.0120(19)	Cu2-$N8_{(pyridyl)}$	2.0149(19)
Cu1-$N3_{(azomethine)}$	1.981(2)	Cu2-$N7_{(azomethine)}$	1.977(2)
Cu1–S1	2.2646(6)	Cu2-S2	2.2556(6)
Cu1-S2	2.7775(7)	C-$N_{(hydrazinic)}$	1.321(6); 1.309(3)
C-S	1.752(3);1.746(3)	C-$N_{(amino)}$	1.355(3); 1.364(3)
N3 -Cu1-Br1	161.74(6)	N7 -Cu2-Br2	158.69(6)
N4-Cu1-S1	163.42(6)	N8-Cu2-S2	163.46(7)
Br1-Cu1-N4	98.98(6)	Br2-Cu2-N8	98.57(7)
Br1 -Cu1-S1	96.46(2)	Br1-Cu2-S2	97.69(2)
N3-Cu1-N4	80.74(8)	N7-Cu2-N8	80.57(8)
N3-Cu1-S1	82.70(6)	N7-Cu2- S2	83.19(5)

τ value	0.028	Cu2-S2-Cu1	85.03(2)
$Cu^{II}(\kappa^3$:N,N,S-L^1-Et)Cl] **8**			
Cu1-Cl1	2.2497(8)	$Cu1\text{-}N1_{(azomethine)}$	1.971(2)
$Cu1\text{-}N3_{(pyridyl)}$	2.039(2)	Cu1-S1	2.2625(9)
C-S	1.743(3)	$C\text{-}N_{(hydrazine)}$	1.330(4)
$C\text{-}N_{(amino)}$	1.334(4)		
S1-Cu1-Cl1	97.14(3)	S1-Cu1-N1	83.32(8)
N1-Cu1-N3	80.68(10)	N3-Cu1-Cl1	98.40(8)
S1-Cu1-N3	163.93(8)	N1-Cu1-Cl1	170.64(8)

S3. ESR spectroscopy

The X-band ESR spectra of microcrystalline samples of complexes **1-9** were recorded to support divalent state of copper(II) and the ESR parameters (g, A and G -exchange parameter) are listed in Table S1. Figures S20-S28 depict the respective ESR spectra of complexes **1-9** respectively. Due to the distortion in geometry and the dipolar broadening induced by the closest neighbors in the crystal lattice, coupling from ^{63}Cu (I = 3/2) nucleus in the parallel and the perpendicular regions is not observed. Complexes **1** and **8** have shown partial ^{63}Cu coupling signals in the II regions and the ESR spectra of **1**, **4** and **8** conform to axial symmetry with the g parameters in the trend : $g_{II} > g_{\perp} > 2$ which implies that $^2B_1$ is the ground state of copper(II) in these complexes. Complexes **3**, **6** and **7** have shown rhombic ESR spectra with g_1, g_2 and g_3 values calculated as : **3**, g_1, 2.372, g_2 = = 2.239, g_3 = 2.102; **6**,

g_1 = 2.218, g_2 =2.090; **7**, g_1= 2.170; g_2 = 2.045; g_3 =2.027. Finally, complexes **2**, **5** and **9** have shown exchange broadened isotropic spectra with the g_{iso} values in the range, 2.072 to 2.084. The exchange interaction between copper centers in the polycrystalline compound is revealed by the geometric parameter G, which is calculated using the equation, G = g_{II}-2.003/$g_{\perp}$-2.003. The G values calculated for complexes **1**$_{(I,Me)}$, **4**$_{(Br,Me)}$, and **8**$_{(Cl, Et)}$ fall in the range, 3.375-4.018 and G < 4 shows exchange interaction in the solid complexes **1** and **8.** Weak interaction is indicated in complex **4**.

Table S2. ESR data of complexes **1-9**[a]

Complex	g-values		g_{iso}	G
1	2.130(g_{II})	2.039($g_{\perp}$)	2.069	3.528
2	-	2.080($g_{\perp}$)	2.080	-
3	g_1 = 2.372, g_3 = 2.102	g_2 = 2.239	2.238	-
4	2.154(g_{II})	2.040($g_{\perp}$)	2.078	4.081
5	-	2.084($g_{\perp}$)	2.084	-
6	g_1 = 2.218	g_2 = 2.090	2.154	-
7	g_1 = 2.170	g_2= 2.045 g_3= 2.027	2.081	-
8	2.138(g_{II})	2.043($g_{\perp}$)	2.075	3.375

9	-	2.072($g_{\perp}$)	2.072	-

[a]A in gauss

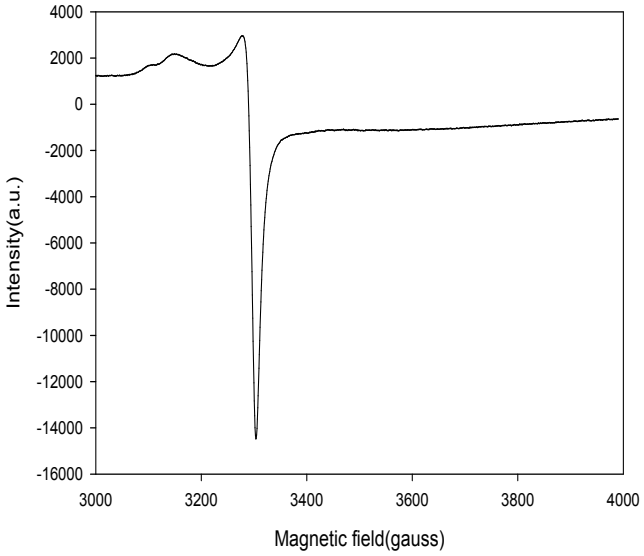

Fig. S2. The X-band ESR spectrum of complex [Cu^{II}(κ^3:N,N,S-L^1-Me)I] **1**

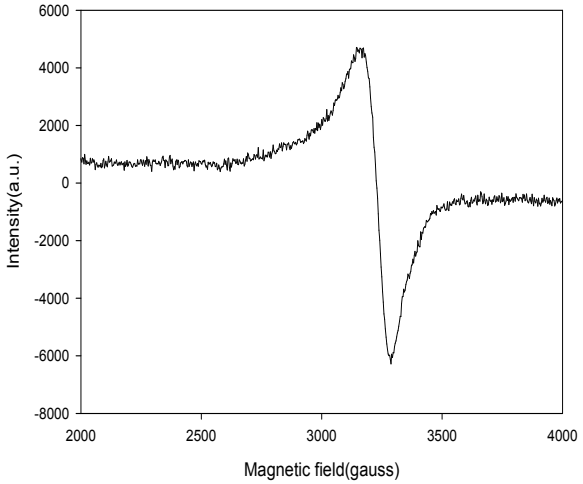

Fig. S3. The ESR spectrum of [Cu_2^{II}(κ^4: N,N,μ-S-L^1-Et)$_2$$I_2$] **2**

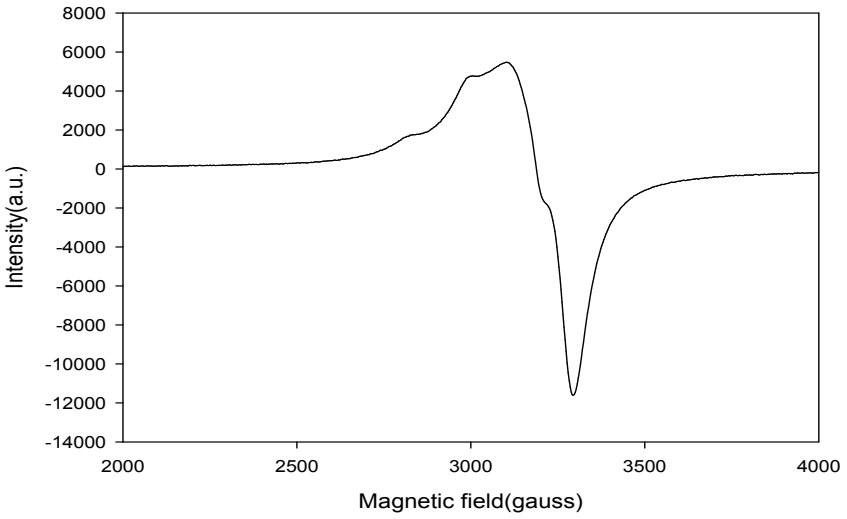

Fig. S4. The ESR spectrum of $[Cu_2^{II}(\kappa^3:N,N,S\text{-}L^1\text{-}Ph)(\kappa^4:N,N,\mu\text{-}S\text{-}L^1\text{-}Ph)I_2]$ **3**

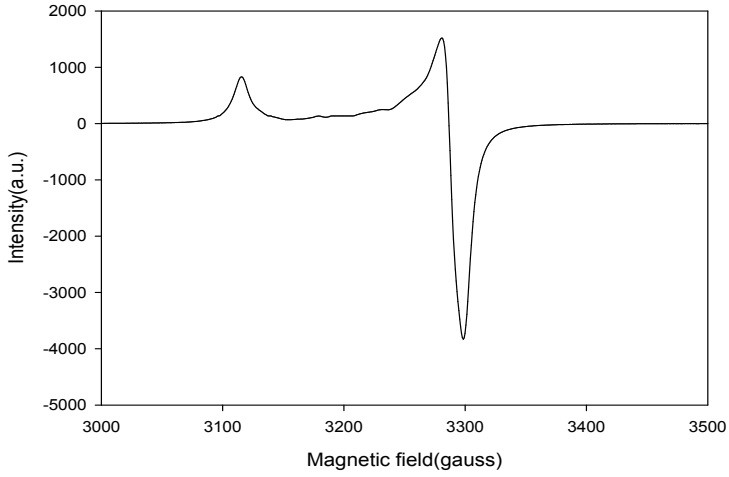

Fig. S5. The ESR spectrum of $[Cu^{II}(\kappa^3:N,N,S\text{-}L^1\text{-}Me)Br]$ **4**

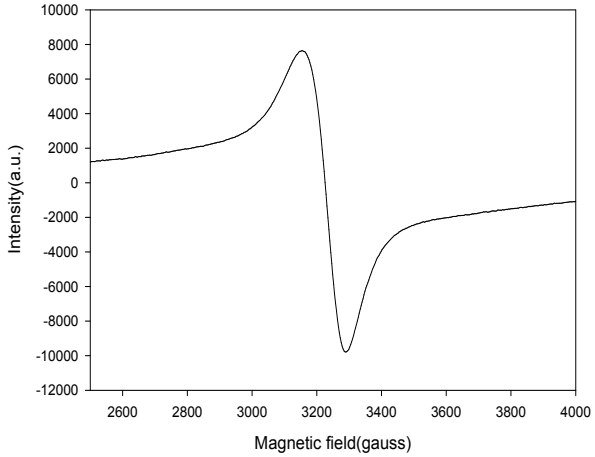

Fig. S6. The ESR Spectrum of $[Cu_2^{II}(\kappa^3:N,N,S\text{-}L^1\text{-}Et)_2Br_2]$ **5**

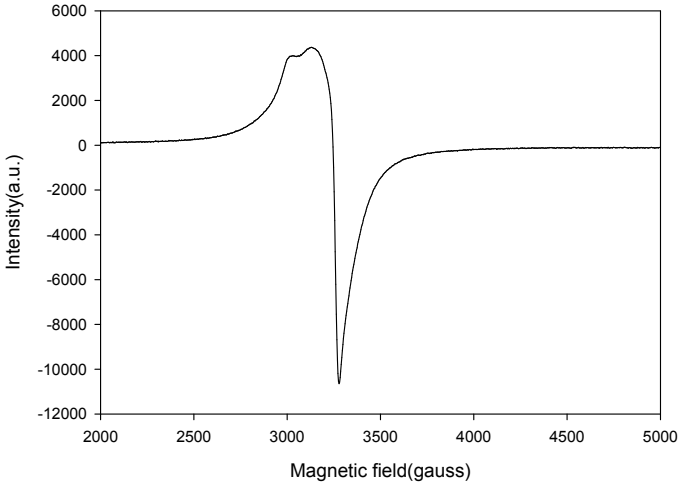

Fig. S7. The ESR spectrum of $[Cu_2^{II}(\kappa^3:N,N,S\text{-}L^1\text{-}Ph)(\kappa^4:N,N,\mu\text{-}S\text{-}L^1\text{-}Ph)Br_2]$ **6**

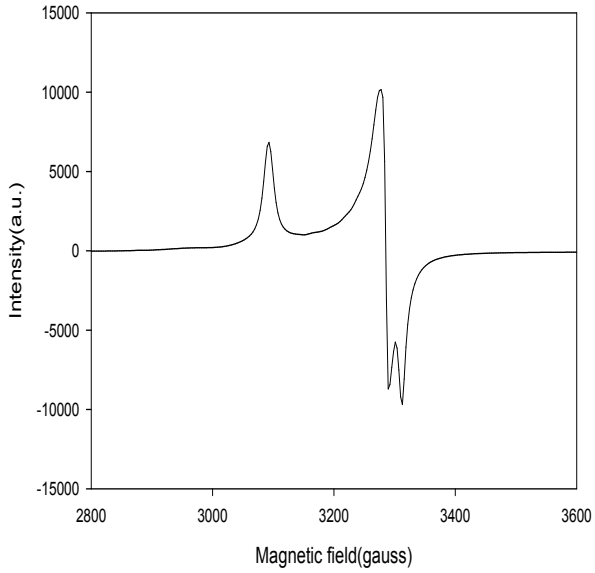

Figure 9

Fig S8. The ESR spectrum of [Cu^{II}(κ^3: N,N,S-L^1-Me)Cl] **7**

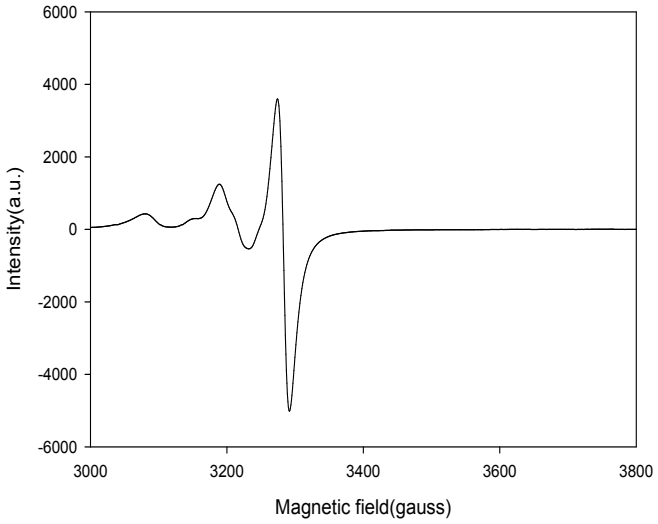

Fig. S9. The ESR spectrum of [Cu^{II}(κ^3: N, N, S-L^1-Et)Cl] **8**

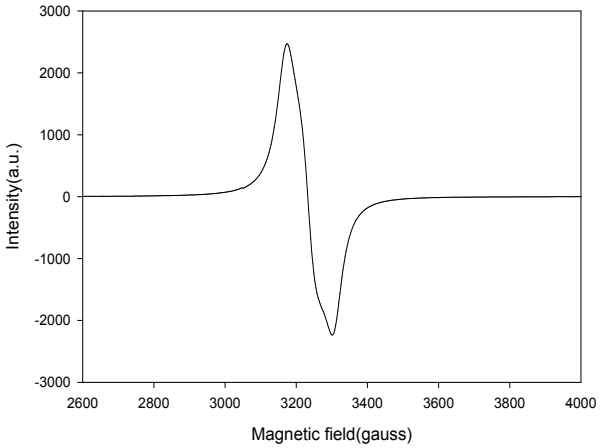

Fig. S10. The ESR spectrum of [Cu^{II}(κ^3:N,N,S-L^1-Ph)Cl] **9**

S4.ESI-mass studies

Various species of complexes

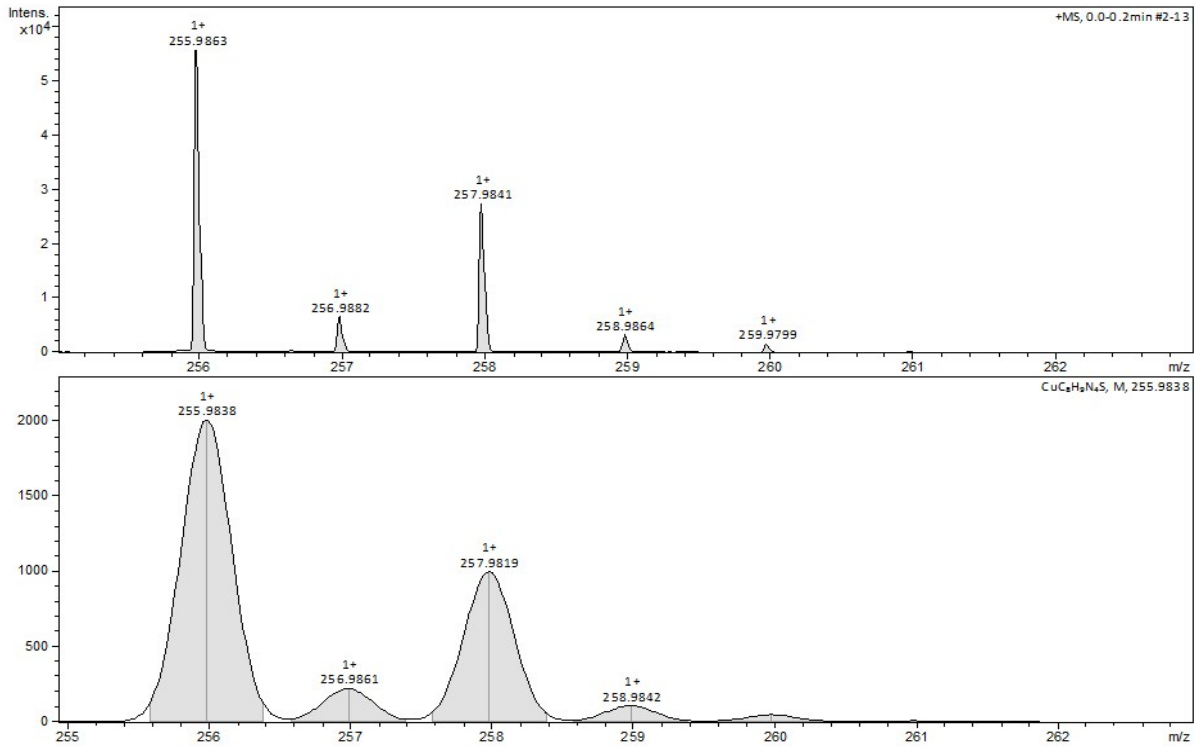

Fig. S11. ESI-mass spectrum of $[Cu(N,N,S\text{-}L^1\text{-}Me)]^+$ species **B** (chemical formula: $CuC_8H_9N_4S$; m/z = calc 255.98,obsd 255.98) with isotropic pattern (Complex **7**)

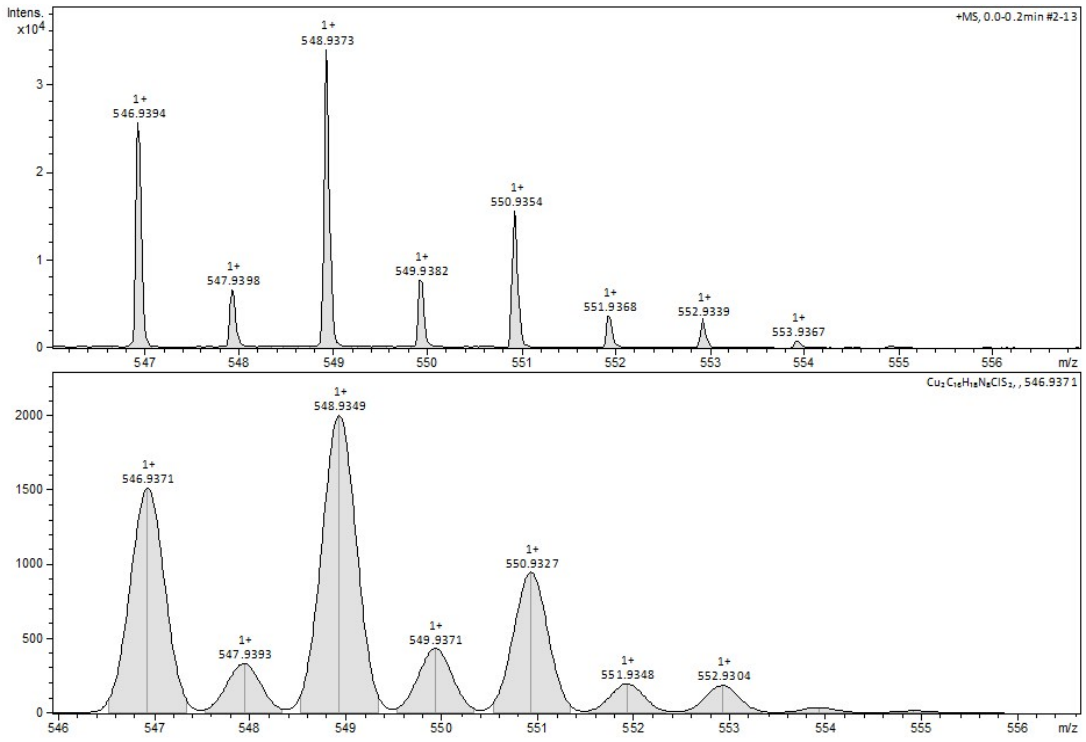

Fig. S12. ESI-mass spectrum of $[Cu_2(N,N,S\text{-}L^1\text{-}Me)_2Cl]^+$ species **C** (chemical formula: $Cu_2C_{16}H_{18}N_8S_2Cl$; m/z = calcd 546.93, obsd 546.94) with isotropic pattern (complex **7**)

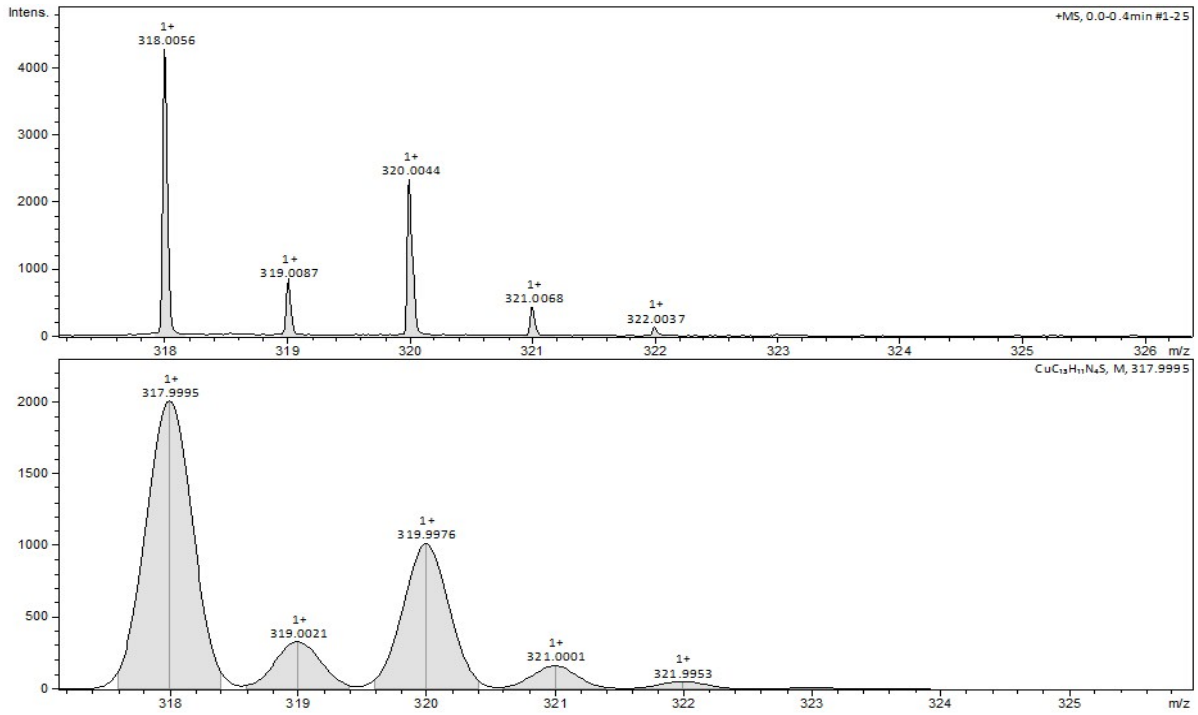

Fig. S13. ESI-mass spectrum of $[Cu(N,N,S\text{-}L^1\text{-}Ph)]^+$, species **B** (chemical formula: $CuC_{13}H_{11}N_4S$; m/z = calc 317.99, obsd 318.00) with isotropic pattern (complex **3**)

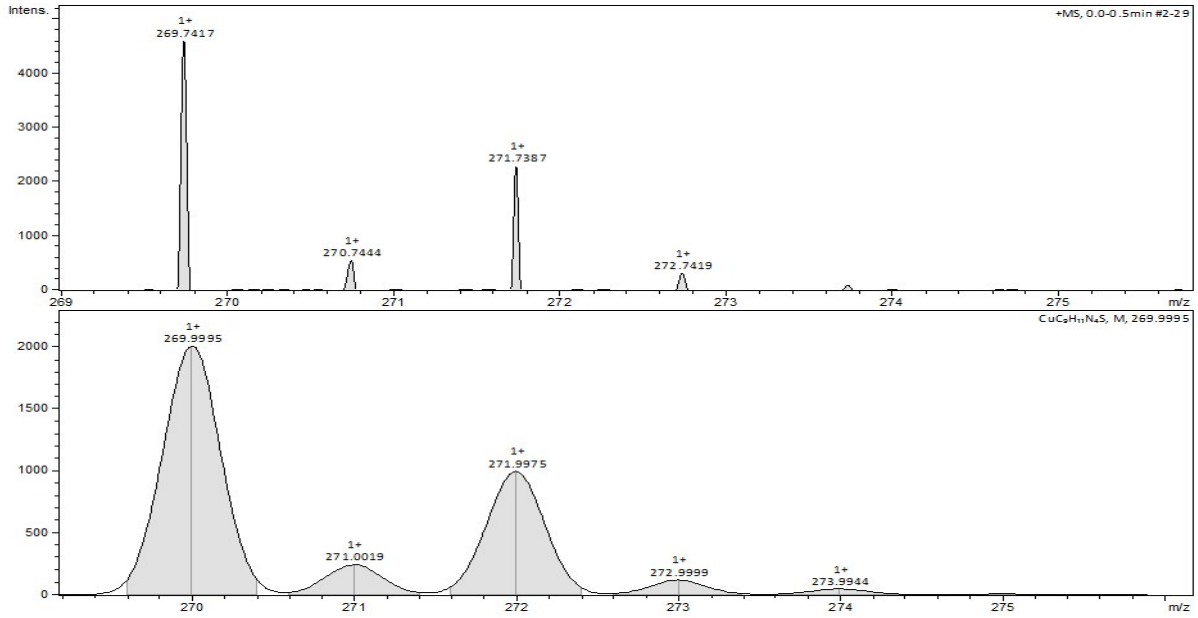

Fig. S14. ESI-mass spectrum of $[Cu(N,N,S\text{-}L^1\text{-}Et)]^+$, species **B** (chemical formula: $CuC_9H_{11}N_4S$; m/z = calcd 269.99, obsd 269.74) with isotropic pattern (complex **5**)

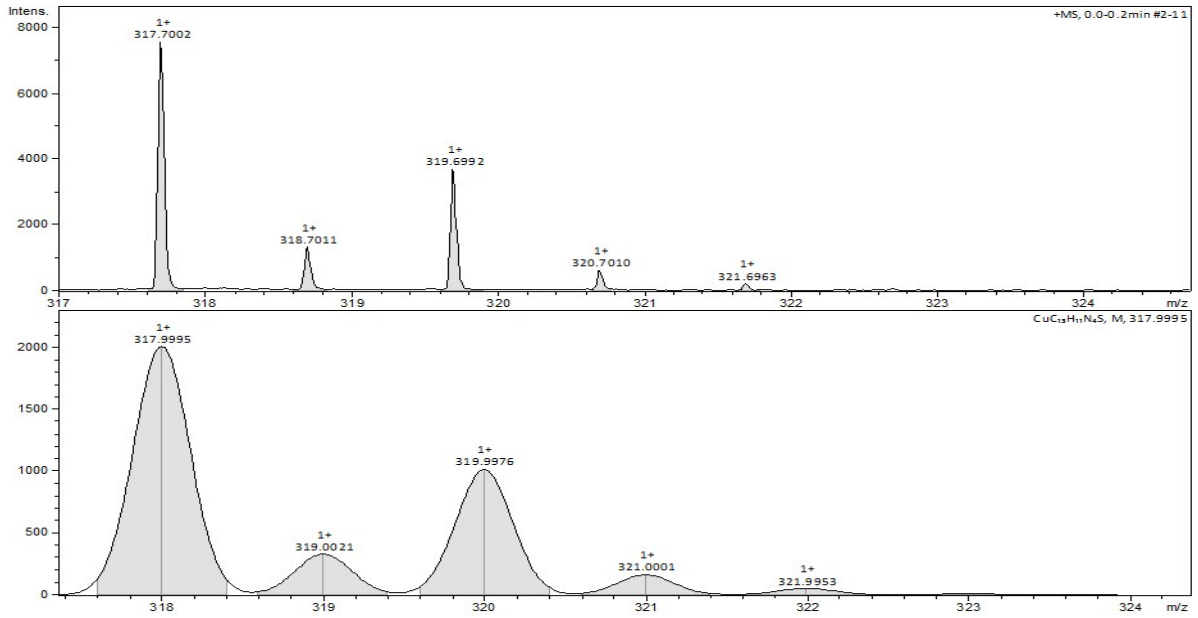

Fig. S15. ESI-mass spectrum of $[Cu(N,N,S\text{-}L^1\text{-}Ph)]^+$, species **B** (chemical formula: $CuC_{13}H_{11}N_4S$; m/z = calcd 317.99, obsd 317.70) with isotropic pattern (complex **6**)

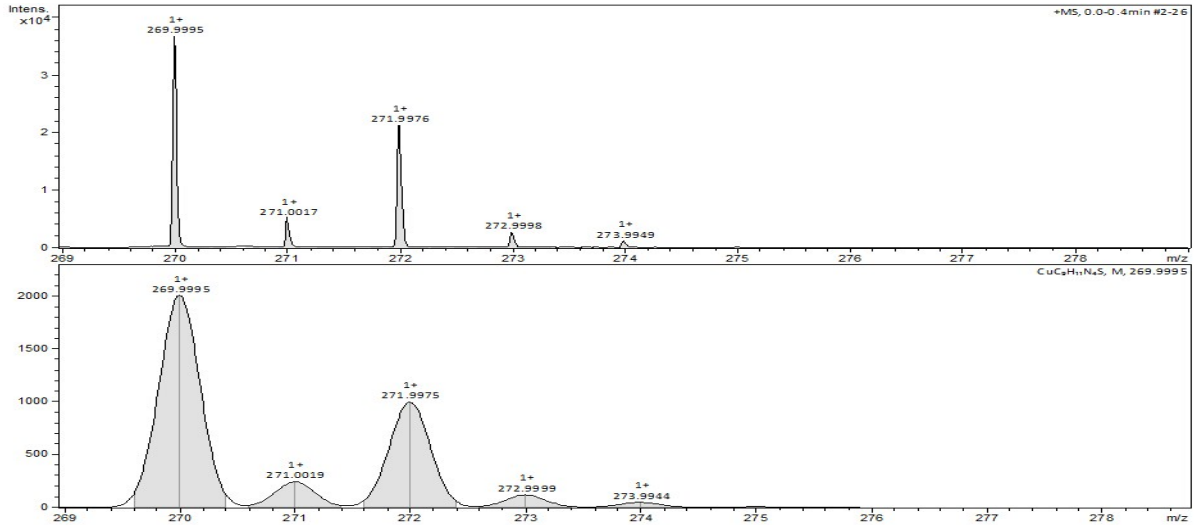

Fig. S16. ESI-mass spectrum of $[Cu(N,N,S\text{-}L^1\text{-}Me)]^+$, species **B** (chemical formula: $CuC_9H_{11}N_4S$; m/z = calcd 269.99, obsd 269.99) with isotropic pattern (complex **8**)

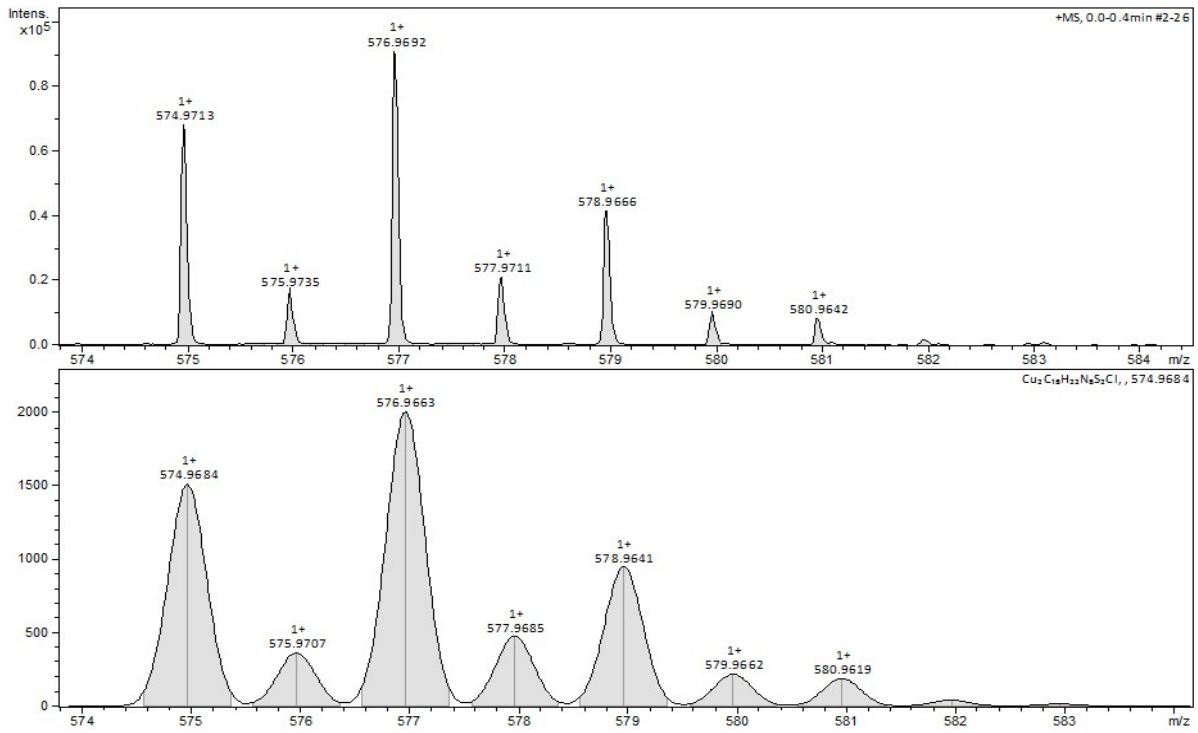

Fig. S17. ESI-mass spectrum of $[Cu_2(N,N,S\text{-}L^1\text{-}Et)_2Cl]^+$ species **C** (chemical formula: $Cu_2C_{18}H_{22}N_8S_2Cl$; m/z = calc 574.96, obsd 574.97) with isotropic pattern (complex **8**)

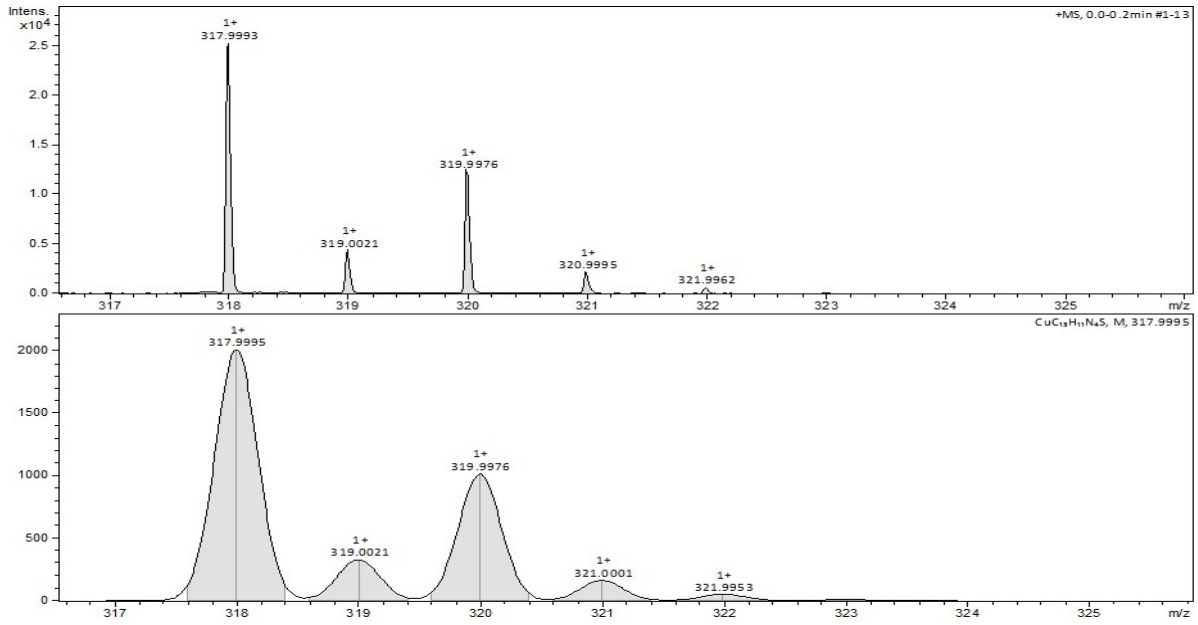

Fig. S18. ESI-mass spectrum of $[Cu(N,N,S\text{-}L^1\text{-}Ph)]^+$ species **B** (chemical formula: $CuC_{13}H_{11}N_4S$; m/z = calcd 317.99, obsd 317.99) with isotropic pattern(complex **9**)

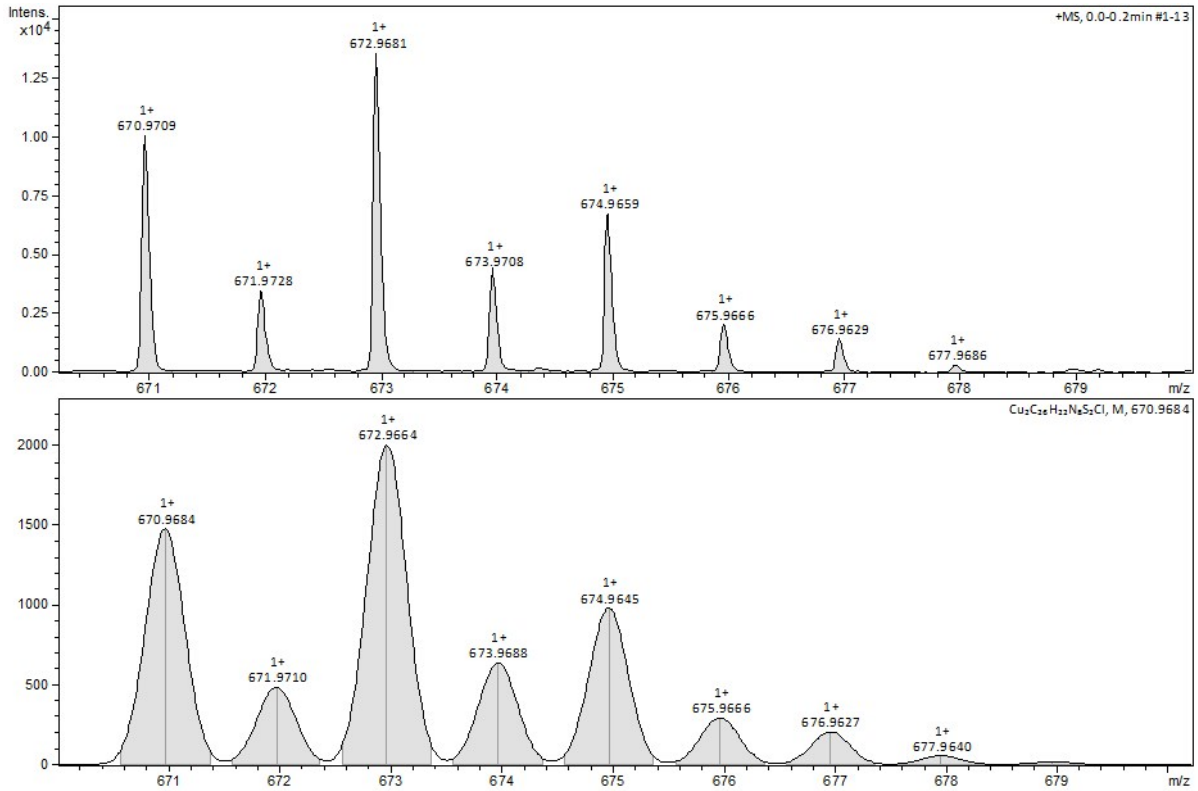

Fig. S19. ESI-mass spectrum of $[Cu_2(L^1\text{-}Ph)_2Cl]^+$ species **C** (chemical formula: $Cu_2C_{26}H_{22}N_8S_2Cl$; m/z = calcd 670.97,obsd 670.97) with isotropic pattern(complex **9**)

S5..UV spectra of complexes

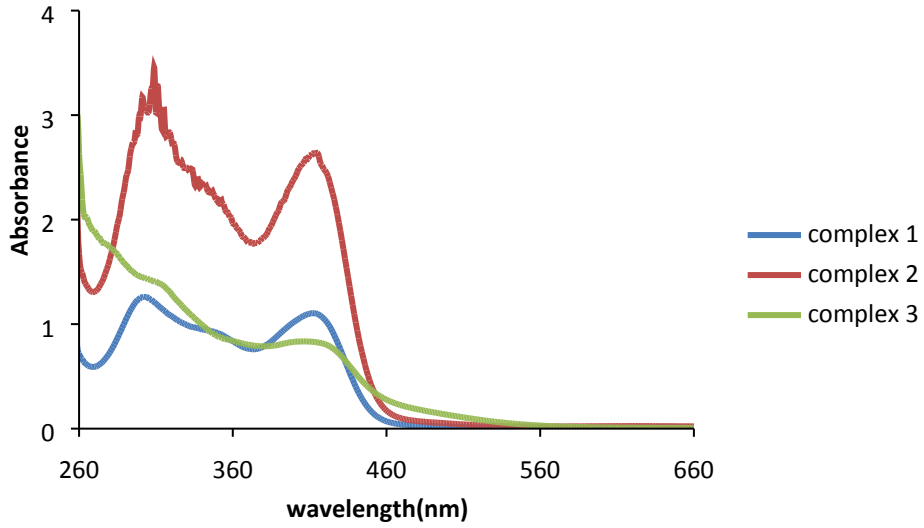

Fig. S20. UV-Spectra of Complexes (**1**, **2** and **3**) at 10^{-4}M in DMSO

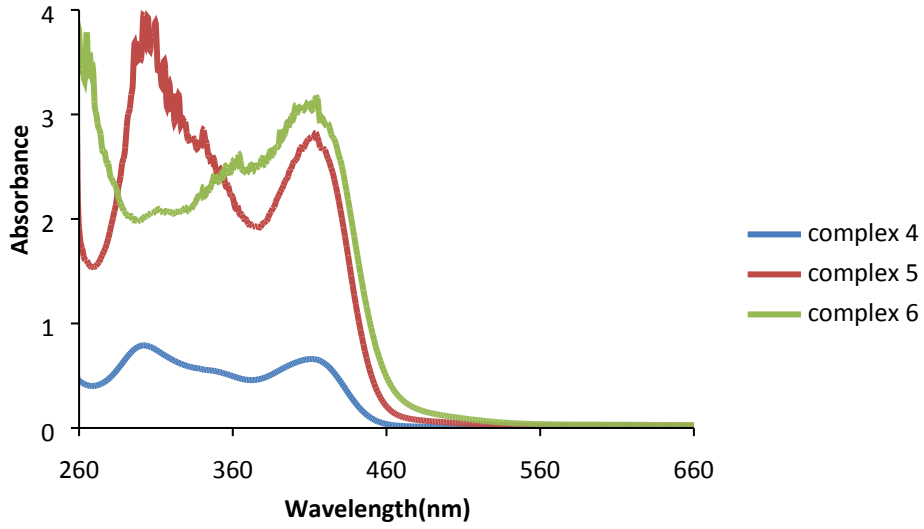

Fig. S21. UV-Spectra of Complexes (**4**, **5** and **6**) at 10^{-4}M in DMSO

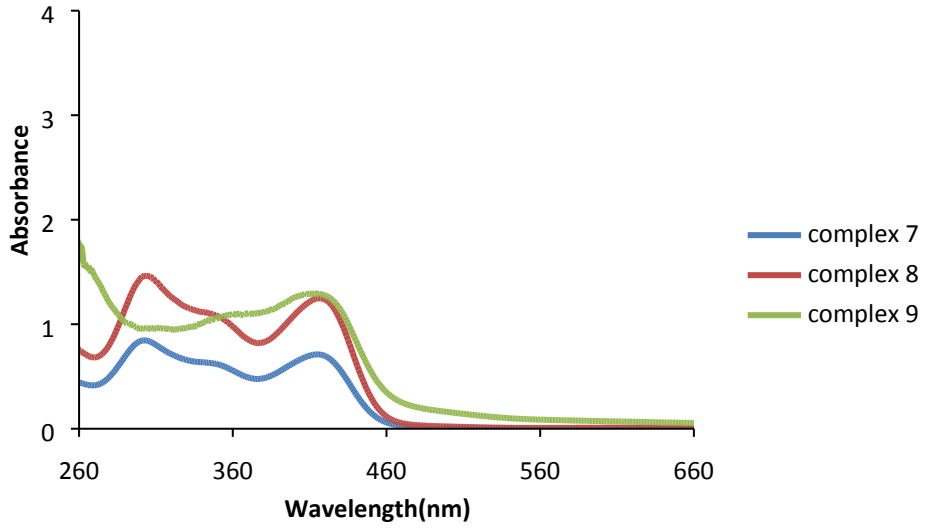

Fig. S 22 UV-Spectra of Complexes (**7**, **8** and **9**) at 10^{-4}M.in DMSO

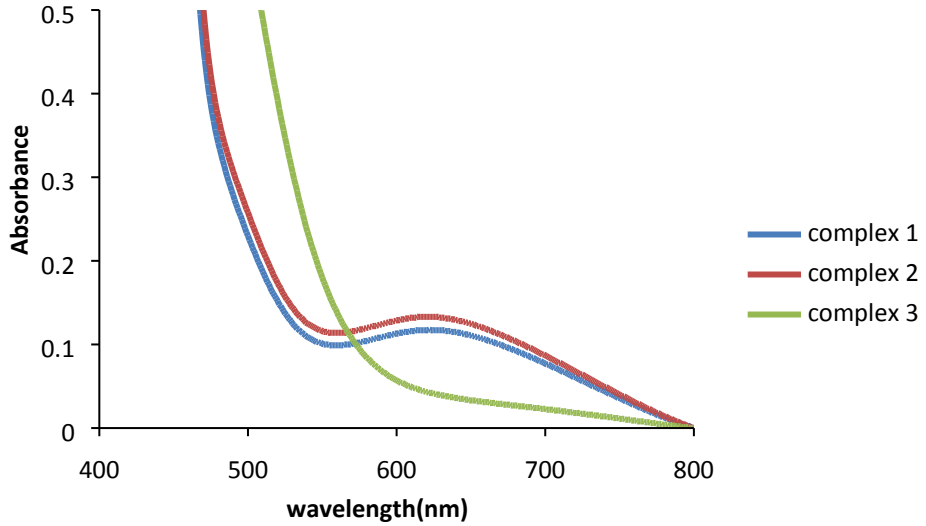

Fig. S23. Electronic absorption spectra of complexes (**1**, **2** and **3**) at 10^{-3}M in DMSO in the visible region.

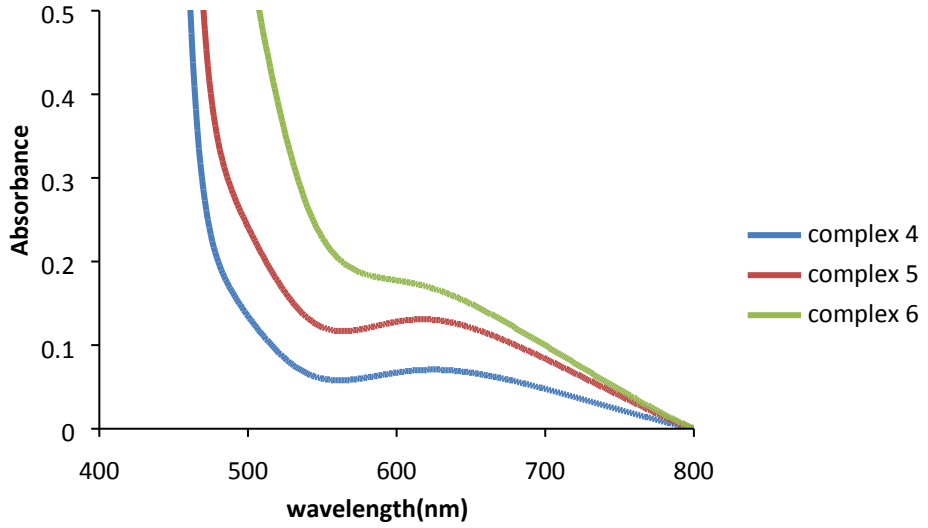

Fig. S24. Electronic absorption spectra of complexes (**4**, **5** and **6**) at 10^{-3}M in DMSO in the visible region.

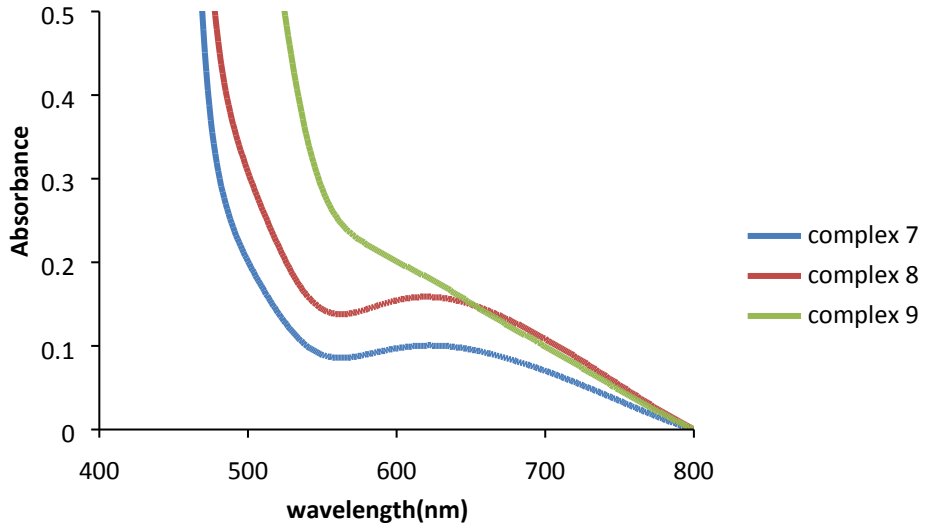

Fig. S 25. Electronic absorption spectra of complexes (**7**, **8** and **9**) at 10^{-3}M in DMSO in the visible region.

4S. Electron absorption spectra of representative compounds to observe effect of solvent and other conditions

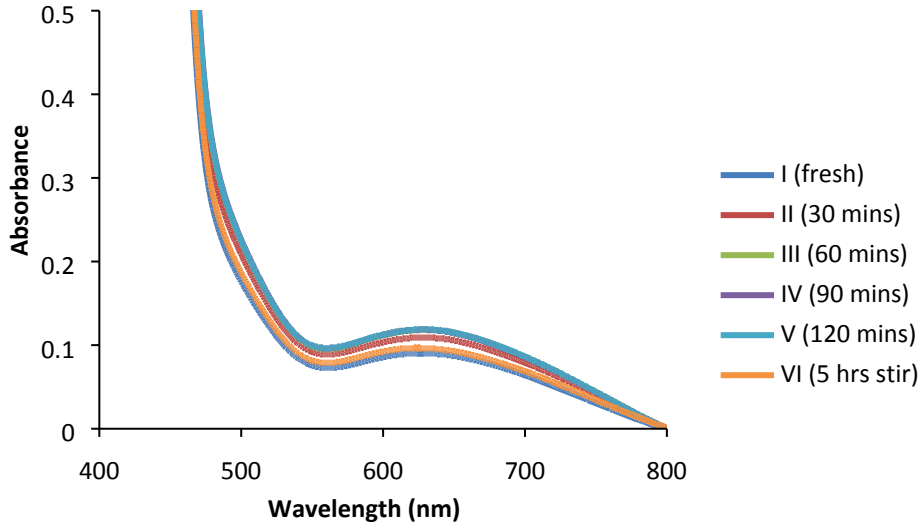

Fig. S26a. Electronic absorption spectra of 10^{-3} M solution of complex **7** in DMSO recorded at different intervals of time : 0 (fresh), 30 mins, 60 mins, 90 mins, 120 mins and after 5hrs strirring

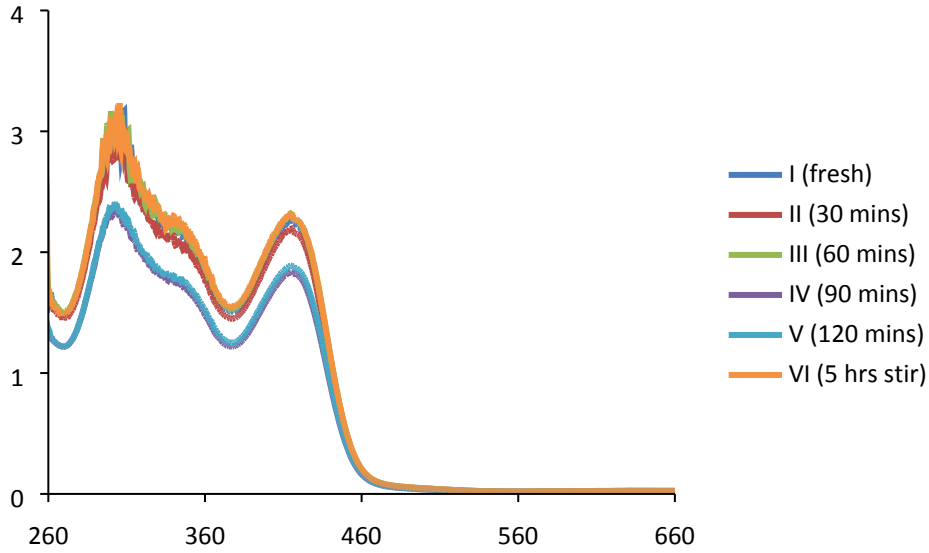

Fig. S26b. Electronic absorption spectra of 10^{-4} M solution of complex **7** in DMSO recorded at different intervals of time : 0 (fresh), 30 mins, 60 mins, 90 mins, 120 mins

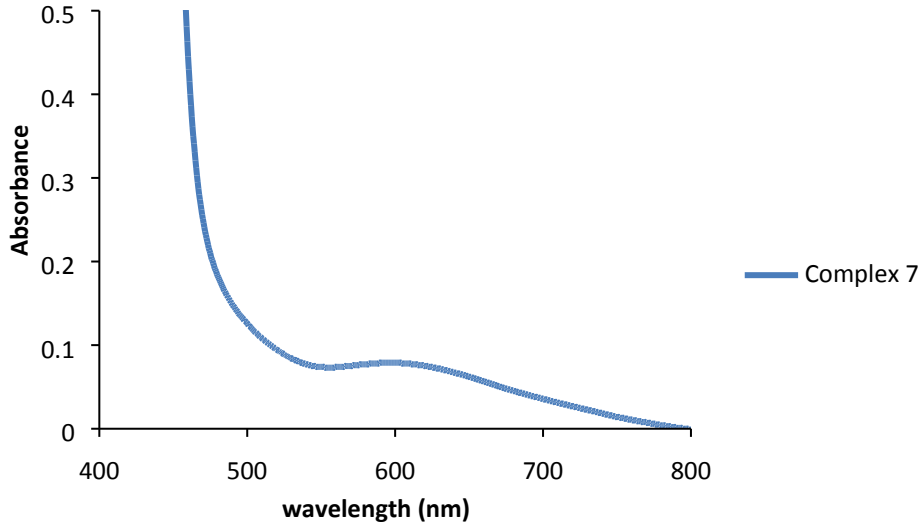

Fig. S27a. Electronic absorption spectrum of 10^{-3} M solution of complex **7** in acetonitrile

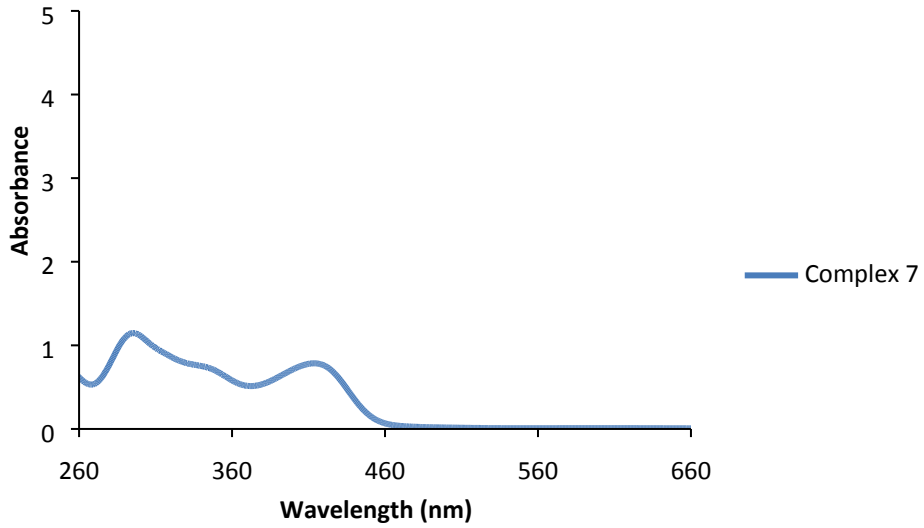

Fig. S27b. Electronic absorption spectrum of 10^{-4} M solution of complex **7** in acetonitrile

S6. Test organisms and inoculum preparation

The reference strains of bacteria and yeasts were obtained from Microbial Type Culture Collection (MTCC), Institute of Microbial Technology (IMTECH), Chandigarh, India while the clinical isolate methicillin resistant *Staphylococcus aureus* (MRSA) was obtained from Post graduate Institute of Medical Education and Research, (PGIMER), Chandigarh, India. Reference strains included Gram positive bacteria: *Staphylococcus aureus* (MTCC-740), *Staphylococcus epidermidis* (MTCC-435), Gram negative bacteria: *Klebisella pneumoniae* (MTCC-530), *Escherichia coli* (MTCC-119), *Salmonella typhimurium* 1 (MTCC-98), *Salmonella typhimurium* 2 (MTCC-1251), *Shigella flexneri* (MTCC-1457), and one yeast strain: *Candida albicans* (MTCC-227). A loopful of isolated bacterial and yeast colonies were inoculated into 5 mL of their respective medium and incubated at 37 °C and 25 °C, respectively, for 4 h. This was used as inoculums after adjusting the turbidity as per Mc Farland turbidity standard. This turbidity is equivalent to approximately 1 to 2 x 10^8 colony forming units per mL (CFU mL^{-1}). The inoculums thus prepared were used for further testing.

S6.1 Antimicrobial screening

A 100 μL of activated test organism (prepared as above) was inoculated onto suitable medium plates by spread plate method. Wells measuring 8 mm in diameter were cut out in the medium using sterilized stainless steel borer. Each well was filled with 0.1 mL of test complex dissolved in DMSO and kept for incubation in an upright position for 18 – 24 h. Sensitivity was measured in terms of diameter of the resultant zone of inhibition. Any organism with a clear zone of inhibition ≤ 12mm was considered to be resistant to the compound.

S6.2 Minimum inhibitory concentration (MIC)

Minimum inhibitory concentration of the selected complex compounds dissolved in DMSO was worked out by the agar dilution method for their antimicrobial activity against the sensitive microorganisms. A stock solution of a complex under investigation of concentration (10 mg mL^{-1}) was prepared and incorporated into Muller Hinton agar medium for bacteria and yeast malt extract medium for yeast. The final concentration of the compound in the medium containing plates ranged from (0.005–1 mg mL^{-1}). These plates were then inoculated with 0.1 mL of the activated bacterial and yeast strains by streaking with a sterile tooth pick. The plates were incubated at 37ºC for bacteria and 25 ºC for yeast for 24 h each. The minimum concentration of the extract causing complete inhibition of the microbial growth was taken as MIC. The results were compared with that of control (i.e. DMSO).

S6.3 Cellular toxicity testing using MTT assay

The biosafety of the test compounds was checked by MTT [3-(4, 5-dimethylthiazol-2-yl)-2, 5-diphenyl tetrazolium bromide] assay [67]. Ten milliliter of sheep blood was taken into injection syringe containing 3 mL of Alsever's solution (anticoagulant) and transferred to sterile centrifuge tubes. The blood was centrifuged at 16,000 rpm at room temperature (25°C) for 20 min so as to separate the plasma from the cells. The supernatant was discarded and 6 mL phosphate buffer saline (PBS) added which was again centrifuged. The blood cells were washed thrice with PBS by centrifugation and the pellet was re-suspended in 6 mL of PBS. Various dilutions of these cells were prepared using PBS and counted with the help of a hemocytometer under a light microscope so as to obtain cells equivalent to 1×10^5 cells/mL. One hundred microlitre (100 µL) of this diluted suspension was added in each well and incubated at 37 °C for overnight. The supernatant was removed carefully and 200 µL of the sample solution (contains 10 mg/mL) was added and incubated further for 24 h. Supernatant

was removed again and added 20 µL MTT solution (5 mg/mL) to each well and incubated further for 3.5 h at 37 °C on orbital shaker at 60 rpm. After incubation, the supernatant was removed without disturbing the cells and 50 µL of DMSO was added to each well to dissolve the formazan crystals. The absorbance was measured at 590 nm using an automated microplate reader (Biorad 680-XR, Japan). The wells with untreated cells served as control. Reduction of MTT can only occur in metabolically active cells, as MTT is converted into formazan crystals and hence the absorbance directly represents the viability of the cells.

% viability = (OD of Treated / OD of Control) x 100. If the percent viability of the blood cells is quite high, then the compounds are non-cytotoxic in nature.

S6.4. Time kill assay

The time kill assay for the selected purified compounds was performed by the viable cell count method (VCC). A stock solution of (1 mg mL^{-1}) was prepared. Five mL of 4 h grown inoculums was adjusted to 0.5 McFarland standards and serially diluted to 10^{-3} with the respective double strength broth medium. An equal volume of each diluted inoculums and the extract to be tested were mixed at their respective predetermined MIC values and incubated at the respective temperature of 25°C for yeast and 37°C for bacteria. At different time intervals viz. 0, 1, 2, 3, 4, upto 24 h, and 0.1 mL of the mixed suspension was spread on suitable agar plates in duplicate and incubated for 24 h at suitable temperature. The mean number of colonies was determined and compared with that of control, in which the compounds were replaced with DMSO.

S6.4.1. Time kill assay graphs

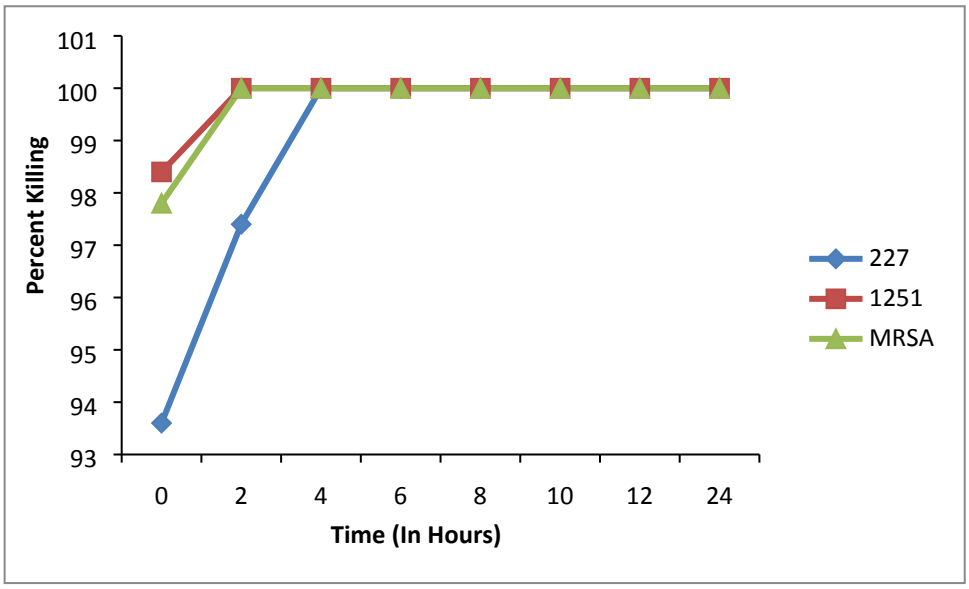

Fig. S28. Complex $[Cu_2^{II}(\kappa^3{:}N,N,S\text{-}L^1\text{-}Et)_2Br_2]$ **5**

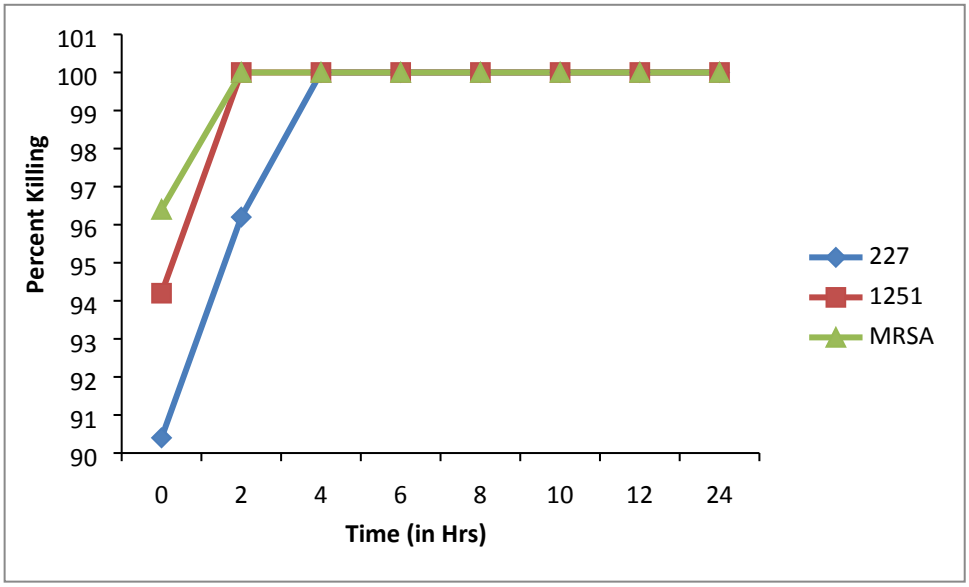

Fig. S29. $[Cu^{II}(\kappa^3{:}\ N,N,S\text{-}L^1\text{-}Et)Cl]$ **8**

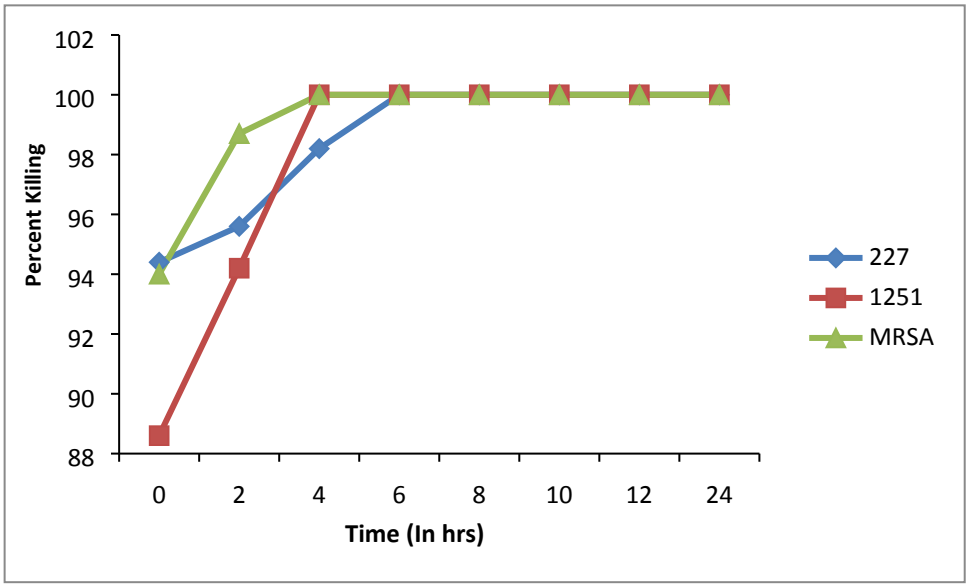

Fig. S30. [$Cu^{II}Br(\kappa^3$-N,N,S- L^2-Me)] **13**

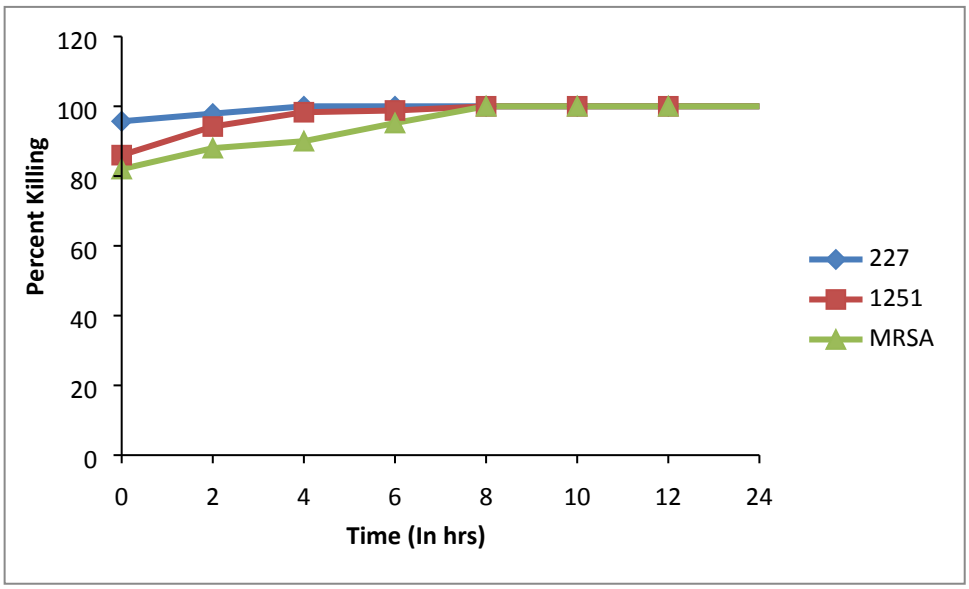

Fig. S31. [$Cu^{II}Cl(\kappa^3$-N,N,S- L^2-Me)] **16**